

Antiferromagnetic domain configurations in patterned LaFeO_3 thin films

This article has been downloaded from IOPscience. Please scroll down to see the full text article.

2007 J. Phys.: Condens. Matter 19 386214

(<http://iopscience.iop.org/0953-8984/19/38/386214>)

View [the table of contents for this issue](#), or go to the [journal homepage](#) for more

Download details:

IP Address: 129.252.86.83

The article was downloaded on 29/05/2010 at 04:43

Please note that [terms and conditions apply](#).

Antiferromagnetic domain configurations in patterned LaFeO₃ thin films

S Czeka¹, F Nolting^{1,4}, L J Heyderman¹, K Kunze² and M Krüger^{3,5}

¹ Paul Scherrer Institut, 5232 Villigen PSI, Switzerland

² Geological Institute, ETH Zürich, 8092 Zürich, Switzerland

³ Physik Institut, Universität Zürich, Winterthurerstrasse 190, 8057 Zürich, Switzerland

E-mail: frithjof.nolting@psi.ch

Received 15 June 2007, in final form 21 July 2007

Published 31 August 2007

Online at stacks.iop.org/JPhysCM/19/386214

Abstract

Photoemission electron microscopy was employed to study the antiferromagnetic domain structure in patterned LaFeO₃ thin films. No influence of the patterning was observed and, using forward scattered electron scanning electron microscopy, a one-to-one correlation of the crystallographic domain structure with the antiferromagnetic domains was found. We deduce that the antiferromagnetic domain structure of thin LaFeO₃ films is determined by the crystallographic domains and this explains why it is not influenced by patterning. Determining the origin of antiferromagnetic domains provides an important step in the understanding of patterned exchange bias systems where antiferromagnetic films play a primary role.

Patterned magnetic thin films are of significant interest due to the novel magnetic effects at reduced lateral dimensions and because of their potential for industrial applications [1]. While we have a detailed knowledge about ferromagnetic (FM) domains in thin films and nanostructures, very little is known about antiferromagnetic (AF) domains [2]. Although, for example, with second harmonic generation [3] or neutron diffraction topography [4] it is possible to investigate the AF domain structure of bulk samples or thick films with a resolution of several micrometers, only a few techniques exist which can image the AF domain structure in thin films and nanostructures [5–7]. However, this information is still being fervently sought, since it will give a better understanding of the complex behavior of nanoscale magnetic devices in which AF thin films are employed. The most prominent application of AF films is in patterned exchange bias systems [8] where the AF layer is coupled to a FM layer. Here the magnetization reversal is determined by the domain configuration in the ferromagnet, which is not only governed by the stray field energy associated with the element size and shape, but also

⁴ Author to whom any correspondence should be addressed.

⁵ Present address: Freiburg Materials Research Centre (FMF), Stefan-Meier-Strasse 21, D-79104 Freiburg, Germany.

very importantly by the domain configuration of the antiferromagnet to which the ferromagnet is coupled [9]. In addition, it has been shown that the size of the exchange bias effect can be influenced by the element size and, although only the FM domain configuration was measured, it was concluded that this was due to a change in the size and arrangement of the AF domains resulting from the patterning [10–13]. However, there are currently no models or measurements which directly reveal exactly what these changes could be or what effects drive them.

In contrast to a ferromagnet, an antiferromagnet has no stray field and one might expect a single domain state to be the thermodynamically stable domain configuration. However, imperfections, such as grains, defects [14] or structural boundaries, act as pinning centers for domain walls so that a multidomain state is often observed. This domain state can even be changed by external strain, as has been shown for single crystalline NiO [15]. Further effects leading to a multidomain state are lattice strain [16], surface roughness [17] and competition between dipolar energy and magnetic anisotropy [2]. One might therefore expect a change in the AF domain configuration resulting from patterning because of the introduction of an additional defect structure and/or a local change of the strain of the film. Aiming to observe such changes, we have studied the AF domain structure in patterned epitaxial LaFeO₃ thin films employing x-ray photoemission electron microscopy (PEEM) combined with x-ray magnetic linear dichroism (XMLD).

For the patterning, three fundamentally different methods were developed to produce square and circular structures in the size range of 0.4–20 μm in the films, or 70 nm wide line defects through individual domains: pre-patterning, where the LaFeO₃ film is grown on a patterned substrate, post-patterning, where the LaFeO₃ film is directly patterned, and ion beam damaging, where the LaFeO₃ film is patterned by damaging areas with a focused ion beam (FIB) to make them nonmagnetic. While the pre-patterning has the advantage that the LaFeO₃ film is not damaged as a result of the patterning process, the post-patterning or the damaging allows measurement of the sample before and after the patterning. Therefore we can distinguish between changes induced by patterning and effects of the sample growth. This was found to be very important since the AF domain size varies strongly between different samples grown with the same conditions [18]. It turns out that we observed no influence of the patterning on the AF domain configuration using these three different patterning methods. In addition, using forward-scattered electron scanning electron microscopy (FSE-SEM), a one-to-one correlation of the AF domains with the crystallographic domain structure was found. This shows that the AF domain structure of thin LaFeO₃ films is determined by the crystallographic domains produced during the film growth, which cannot be changed by patterning.

The epitaxial LaFeO₃ films, 25 nm thick, were grown on SrTiO₃ (STO) (001) substrates using pulsed laser deposition (PLD) and capped with 1 nm Pt (details are published elsewhere [18]). For the pre-patterning, electron beam lithography was employed in combination with ion milling to produce patterned STO substrates. The post-patterning was carried out using electron beam lithography with ion milling (1 keV Ar ions with a fluence around 10^{21} cm^{-2}). As a result, the LaFeO₃ between the structures is completely removed. In both cases a patterned Cr film was employed as a hard mask. The damaging was performed using a FIB and the dose (30 kV Ga ions with fluence around 10^{18} cm^{-2}) was chosen such that the LaFeO₃ between the structures was completely damaged with removal of only a few monolayers, so maintaining a flat surface. The AF domain configuration was determined with an Elmitec PEEM at the SIM Beamline. Dividing two images taken with photon energies corresponding to the multiplet structure of the Fe L₃ or L₂ absorption edge, an XMLD image is obtained. All of the XMLD images shown were taken with linearly polarized x-rays coming from the right with respect to the image, and with the *E*-vector oriented in the surface plane. For this case a bright (dark) XMLD image intensity means a more parallel (perpendicular) spin

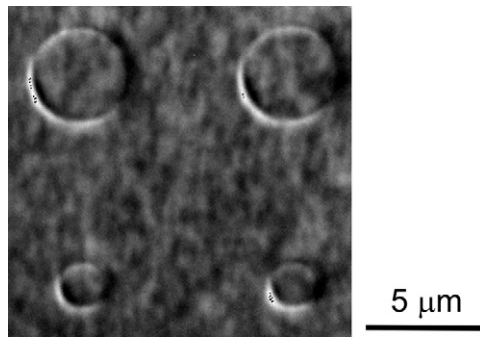


Figure 1. XMLD image of a pre-patterned thin LaFeO_3 film. The patterns were created by thin film deposition on a pre-patterned STO substrate prepared by electron beam lithography with ion milling. The disks shown here have a diameter of 4 and $1.7 \mu\text{m}$. The white and black crescent shapes at the border of the disks are imaging artifacts due to topography. The dark and bright areas are small AF domains (around 300 nm), which have the same appearance on the disks and in the surrounding area.

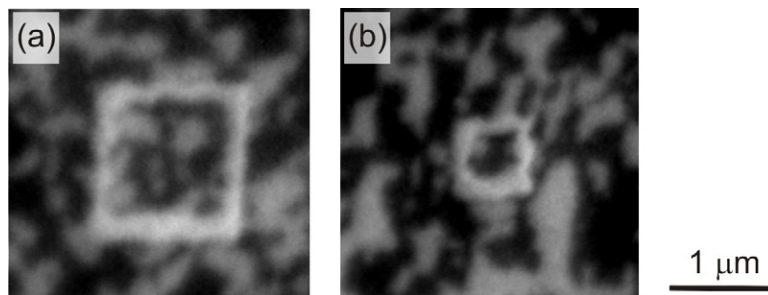


Figure 2. XMLD images of post-patterned thin LaFeO_3 films. The patterns were created by post-patterning using electron beam lithography with ion milling. Examples of a $1 \mu\text{m}$ and 400 nm structure are given in (a) and (b), respectively. The white lines correspond to the removed LaFeO_3 material resulting in square structures in the continuous film. The irregular shape of these white lines is an effect resulting from the processing. The bright and dark regions everywhere else correspond to different AF domains, which have the same appearance in the square structures and in the surrounding area.

axis orientation with respect to the E -vector [18]. The crystallographic domain configuration was measured with FSE-SEM, which is sensitive to the relative crystalline orientation [19].

We have studied the AF domain configuration in all of the differently patterned LaFeO_3 films. For the pre-patterned films no difference is visible between the AF domains on the structure and the surrounding area. Examples of disks with diameters of 4 and $1.7 \mu\text{m}$ are given in figure 1, where it can be seen that the AF domains are much smaller (around 300 nm) than the structure. The effects of structuring might become visible when they have a comparable size. However, for the pre-patterned sample it was not possible to grow films with larger AF domains, which was probably due to an increased surface roughness of the substrate produced during the ion milling.

For the films grown on pristine STO substrates, we could obtain much larger AF domains with $>1 \mu\text{m}$ sizes. Examples of such films, post-patterned with a $1 \mu\text{m}$ and a 400 nm square structure, are given in figures 2(a) and (b), respectively. XMLD images of various structure sizes, from 400 nm up to several micrometers (not shown), have shown consistently that the

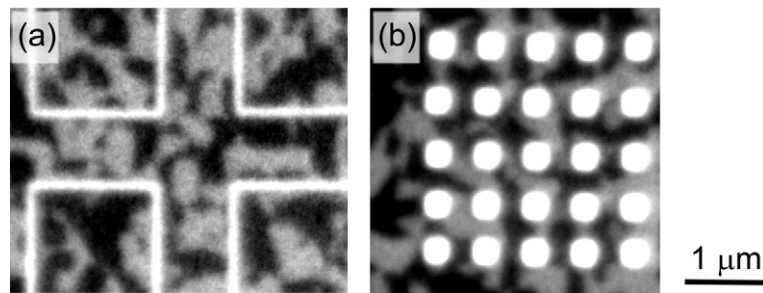


Figure 3. XMLD images of post-patterned thin LaFeO_3 films. The patterns were created by FIB lithography. The white lines in (a) correspond to the damaged nonmagnetic LaFeO_3 material creating rectangular structures in the film. The bright and dark regions everywhere else are different AF domains. In addition, an example of an antidot array with a period and size of $1 \mu\text{m}$ and 500 nm is given (b). In all cases the AF domain configuration remained unaffected by the patterning.

appearance of the AF domains in the post-patterned square structures is the same as in the surrounding film and hence is unaffected by the patterning.

In the third patterning approach employing a FIB, the AF film was patterned by ion damaging rather than removal of the surrounding regions. In figure 3(a) the white lines correspond to the damaged nonmagnetic LaFeO_3 material forming rectangular structures such as squares and crosses. The bright and dark regions are different AF domains which are $\approx 1 \mu\text{m}$ in size and do not appear to be affected by the shape of the structures which have been created with the FIB. Furthermore, the white lines can be considered to be narrow line defects, here with a width of 70 nm , and when such a line defect passes through a single domain the domain shape is not affected. We also produced an array of periodic nonmagnetic defects, often referred to as antidots, with different periods and sizes. The antidots appear as white disks in figure 3(b), having a period of $1 \mu\text{m}$, with the antidot size equal to the antidot separation. The antidots do not appear to affect the AF domains in any way, neither acting as pinning centres nor changing the shape of the domains. For all three patterning approaches, we cannot find any indication of an affect on the AF domain configuration due to the patterning. It should be noted that XMLD is not sensitive to 180° AF domains and therefore we should not expect to see any variation of this domain type [14]. Nevertheless it is sensitive to any changes of the AF spin axis orientation which might result from the patterning.

In order to exclude that the domain configuration after patterning is trapped in a local energy minimum, i.e. that there is an influence of the patterning which could be seen if the energy barrier were overcome, we heated the sample above the Néel temperature (565 K). Figure 4 shows how the XMLD contrast measured in a post-patterned film (left) vanishes at 600 K (middle) and is completely recovered upon cooling to room temperature (right). Therefore the AF domain configuration remains unaffected even after heat treatment. In addition to the domain configuration, we have determined the AF spin orientation in the post-patterned sample (figure 2) for AF domains in the square structure and in the surrounding film. The AF spin orientation was found to be the same as that obtained for the initial continuous layers [18]. We measured four orientations of the AF domains; their spin axes exhibit four-fold in-plane symmetry and are canted 20° out-of-plane.

The question of why we are unable to influence the AF domain structure via patterning can be answered by observing the correlation between the AF and crystallographic domain structure in thin LaFeO_3 films. A comparison of the orientation contrast image taken with the FSE-SEM and the XMLD image taken with the PEEM is given in figure 5. Similar studies were

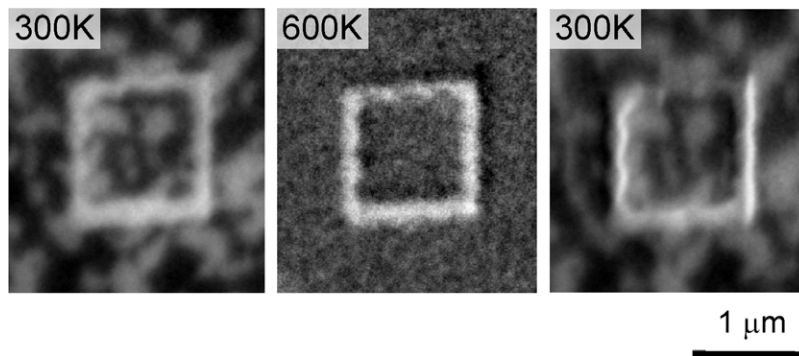


Figure 4. XMLD images taken during a heating–cooling cycle of a post-patterned LaFeO_3 film: at 300 K after the post-patterning (left), above the Néel temperature at 600 K (middle) and back at 300 K after cooling down (right). The XMLD contrast disappears above T_N , and is completely recovered upon cooling to room temperature.

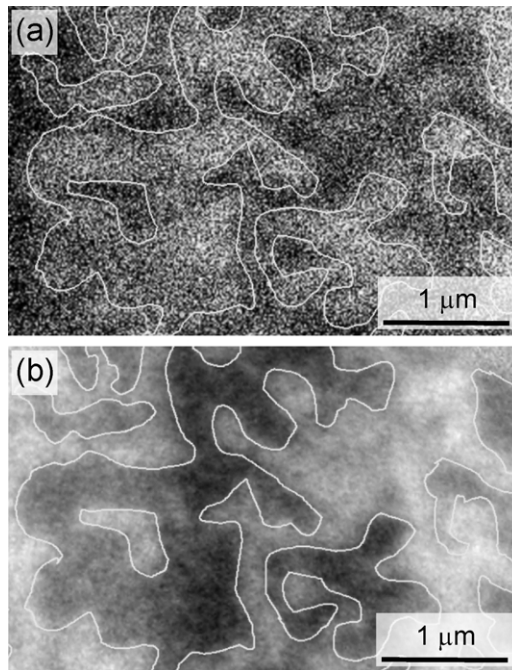


Figure 5. (a) Orientation contrast image measured with FSE-SEM. The bright and dark areas represent twinned crystallographic domains of the thin LaFeO_3 film with mutually perpendicular c -axis orientation. (b) XMLD image measured with PEEM. Bright and dark regions represent two mutually perpendicular in-plane projections of the spin axis. The outlines emphasize the one-to-one correlation between both images. They were first drawn on the XMLD image using the AFM domains as a guide and subsequently overlaid on the FSE-SEM image.

performed comparing PEEM and transmission electron microscope (TEM) images [5, 20], but the same sample position could not be measured with both microscopes. With the help of the structures in one of the post-patterned LaFeO_3 films, we were able to measure the orientation contrast image and XMLD image at the very same sample position. The orientation contrast

image shown in figure 5(a) consists of bright and dark regions which are reversed after a 90° rotation about the surface normal. For thin LaFeO_3 films grown on $\text{STO}(001)$, the origin of the orientation contrast is twinned crystallographic domains with mutually perpendicular c -axis orientations, both lying in-plane. In the XMLD image shown in figure 5(b), bright and dark regions represent two mutually perpendicular in-plane projections of the spin axis. The outlines in figures 5(a) and (b) emphasize the fact that there is a one-to-one correlation between both images, providing experimental proof for the direct correspondence between the antiferromagnetic and the crystallographic domains in LaFeO_3 . Therefore in this system it is the crystalline structure which determines the AF domain configuration and since the crystallographic structure is not influenced by the patterning, the AF domain structure also remains unaffected.

In conclusion, we have shown that patterning of thin LaFeO_3 films does not influence the AF domain configuration observed by x-ray PEEM, even when the patterns are of comparable size. In addition, we revealed by comparing FSE-SEM and PEEM images that the AF domains are directly coupled to the crystallographic structure. Therefore for thin LaFeO_3 films, the crystalline domains are the intrinsic origin of the AF domains, which explains why no change in the AF structure was observed in patterned LaFeO_3 films. Extrapolating our results to patterned exchange bias systems, our findings clearly show that for LaFeO_3 it is not modifications to the AF domains resulting from the patterning that will drive any changes in the magnetization reversal. Quite the opposite: the crystalline domains will try to maintain the already existing antiferromagnetic domain structure. Therefore in order to understand the magnetization reversal, not only should the stray field energy associated with the ferromagnet be taken into account, but also the interaction with the existing AF domains. In order to determine the energetics of these complex multilayer systems, it is therefore important to comprehend the magnetic behavior of the individual layers. However, while the patterned ferromagnets are well understood not much is known about patterned antiferromagnets. Our work is an important step towards closing this gap.

Acknowledgments

We gratefully acknowledge the support from M Horisberger, A Weber and P W Willmott with sample fabrication and analysis. This work was supported by the Swiss National Science Foundation, and part of this work was performed at the Swiss Light Source, Paul Scherrer Institut, Villigen, Switzerland.

References

- [1] Martin J I, Nogués J, Liu K, Vincent J L and Schuller I K 2003 *J. Magn. Magn. Mater.* **256** 449
- [2] Deng D S, Jin X F and Tao R B 2002 *Phys. Rev. B* **65** 132406
- [3] Fiebig M, Lottermoser Th, Pavlov V V and Pisarev R V 2003 *J. Appl. Phys.* **93** 6900
- [4] Beruchel J 1993 *Physica B* **192** 79
- [5] Scholl A, Stöhr J, Lüning J, Seo J W, Fompeyrine J, Siegwart H, Locquet J-P, Nolting F, Anders S, Fullerton E E, Scheinfein M R and Padmore H A 2000 *Science* **287** 1014
- [6] Hillebrecht F U, Ohldag H, Weber N B, Bethke C, Mick U, Weiss M and Bahrtdt J 2001 *Phys. Rev. Lett.* **86** 3419
- [7] Evans P G, Isaacs E D, Aepli G, Cai Z and Lai B 2002 *Science* **295** 1042
- [8] Nogués J, Sort J, Langlais V, Skumryev V, Suriñach S, Muñoz J S and Baró M D 2005 *Phys. Rep.* **422** 65
- [9] Sort J, Hoffmann A, Chung S-H, Buchanan K S, Grimsditch M, Baró M D, Dieny B and Nogués J 2005 *Phys. Rev. Lett.* **95** 067201
- [10] Wang Y J and Lai C H 2001 *J. Appl. Phys.* **89** 7537
- [11] Shen Y T, Wu Y H, Xie H, Li K B, Qiu J J and Guo Z B 2002 *J. Appl. Phys.* **91** 8001

-
- [12] Sort J, Dieny B, Fraune M, Koenig C, Lunnebach F, Beschoten B and Güntherodt G 2004 *Appl. Phys. Lett.* **84** 3696
- [13] Baltz V, Sort J, Rodmacq B, Dieny B and Landis S 2004 *Appl. Phys. Lett.* **84** 4923
- [14] Nowak U, Usadel K D, Keller J, Miltnéyi P, Beschoten B and Güntherodt G 2002 *Phys. Rev. B* **66** 014430
- [15] Slack G A 1960 *J. Appl. Phys.* **31** 1571
- [16] Finazzi M and Altieri S 2003 *Phys. Rev. B* **68** 054420
- [17] Malozemoff A P 1988 *J. Appl. Phys.* **63** 3874
- [18] Czekaj S, Nolting F, Heyderman L J, Willmott P R and van der Laan G 2006 *Phys. Rev. B* **73** 020401(R)
- [19] Mauler A, Bystricky A, Kunze K and Mackwell S 2000 *J. Struct. Geol.* **22** 1633
- [20] Seo J W, Dieker C, Fompeyrine J, Siegwart H and Locquet J-P 2006 *Int. J. Mater. Res.* **97** 943